Bmi-1 promotes neural stem cell self-renewal and neural development but not mouse growth and survival by repressing the p16^{Ink4a} and p19^{Arf} senescence pathways

Anna V. Molofsky, Shenghui He, Mohammad Bydon, Sean J. Morrison,[1] and Ricardo Pardal

Howard Hughes Medical Institute, and Departments of Internal Medicine and Cell and Developmental Biology, University of Michigan, Ann Arbor, Michigan 48109-0934, USA

***Bmi-1* is required for the post-natal maintenance of stem cells in multiple tissues including the central nervous system (CNS) and peripheral nervous system (PNS). Deletion of *Ink4a* or *Arf* from *Bmi-1*$^{-/-}$ mice partially rescued stem cell self-renewal and stem cell frequency in the CNS and PNS, as well as forebrain proliferation and gut neurogenesis. *Arf* deficiency, but not *Ink4a* deficiency, partially rescued cerebellum development, demonstrating regional differences in the sensitivity of progenitors to p16^{Ink4a} and p19^{Arf}. Deletion of both *Ink4a* and *Arf* did not affect the growth or survival of *Bmi-1*$^{-/-}$ mice or completely rescue neural development. Bmi-1 thus prevents the premature senescence of neural stem cells by repressing *Ink4a* and *Arf*, but additional pathways must also function downstream of Bmi-1.**

Supplemental material is available at http://www.genesdev.org.

Received January 19, 2005; revised version accepted April 27, 2005.

Stem cells must persist throughout adult life in numerous tissues in order to replace the mature cells that are lost to turnover, injury, or disease. The mechanism by which stem cells persist throughout life involves self-renewal—stem cell divisions that generate one or two daughter stem cells (Morrison et al. 1997; Molofsky et al. 2004). Stem cells self-renew post-natally in numerous tissues, including the central nervous system (CNS) (Maslov et al. 2004), peripheral nervous system (PNS) (Kruger et al. 2002), and hematopoietic system (Harrison 1979; Morrison et al. 1996).

The polycomb family transcriptional repressor Bmi-1 is required for the self-renewal and post-natal maintenance of hematopoietic stem cells (Lessard and Sauvageau 2003; Park et al. 2003) and neural stem cells from the CNS and PNS (Molofsky et al. 2003). In each tissue *Bmi-1*$^{-/-}$ stem cells form in normal numbers and appear to differentiate normally, but exhibit a post-natal self-renewal defect that leads to their depletion by early adulthood. *Bmi-1* tends to be turned off as cells differentiate (Lessard et al. 1998) and is not required for the proliferation of all cells (Molofsky et al. 2003). Bmi-1 functions as part of a protein complex that maintains gene silencing by regulating chromatin structure (Valk-Lingbeek et al. 2004). Except for a mild skeletal transformation, *Bmi-1*$^{-/-}$ mice are normal in size and appearance at birth (van der Lugt et al. 1994). However, they exhibit progressive post-natal growth retardation and die by early adulthood with signs of hematopoietic failure (hypocellular bone marrow) and neurological abnormalities (seizures and ataxia) (van der Lugt et al. 1994).

Bmi-1$^{-/-}$ mice develop several specific neural abnormalities. The rate of proliferation in the forebrain subventricular zone (SVZ; where CNS stem cells undergo neurogenesis), is reduced by post-natal day 30 (P30) when stem cell depletion becomes severe (Molofsky et al. 2003). The cerebellum also fails to develop normally, partly because *Bmi-1* is required for the proliferation of granule precursor cells (Leung et al. 2004). Finally, adult *Bmi-1*$^{-/-}$ mice exhibit fewer neurons in the myenteric plexus of the gut as the neural crest stem cells (NCSCs) in this region of the post-natal PNS become depleted (Molofsky et al. 2003). These defects indicate that the pathways regulated by Bmi-1 have important consequences for neural development.

Bmi-1 represses transcription at the *Ink4a–Arf* locus (Jacobs et al. 1999a,b), which encodes two inhibitors of cell proliferation (Sherr 2001). *Ink4a* encodes p16^{Ink4a}, a cyclin-dependent kinase inhibitor that promotes Rb activation. *Arf* encodes p19^{Arf}, which promotes p53 activation. p16^{Ink4a} and p19^{Arf} are induced in cultured primary cells and can cause these cells to senesce (for review, see Lowe and Sherr 2003). Bmi-1 overexpression can prevent senescence and extend the replicative lifespan of primary cells by reducing p16^{Ink4a} and p19^{Arf} expression (Jacobs et al. 1999a; Dimri et al. 2002; Itahana et al. 2003). Deletion of *Ink4a–Arf* from *Bmi-1*$^{-/-}$ mice rescues the ability of mouse embryonic fibroblasts to proliferate in culture and at least partially rescues defects in cerebellum development (Jacobs et al. 1999a). p16^{Ink4a} expression is elevated in *Bmi-1*$^{-/-}$ neural stem cells and deletion of *Ink4a* from *Bmi-1*$^{-/-}$ mice partially rescues neural stem cell self-renewal in culture (Molofsky et al. 2003).

To test whether *Ink4a* deletion rescues stem cell frequency or neural development in *Bmi-1*$^{-/-}$ mice, and whether p19^{Arf} also mediates part of the effect of Bmi-1 on stem cell function or neural development, we have generated compound mutant mice that lack *Bmi-1* (van der Lugt et al. 1994) and/or *Ink4a* (Sharpless et al. 2001), *Arf* (Kamijo et al. 1997), or *Ink4a–Arf* (Serrano et al. 1996). Our results indicate that the repression of *Ink4a* and *Arf* each represent major mechanisms by which Bmi-1 promotes neural stem cell self-renewal and neural development. The post-natal maintenance of neural stem cells depends upon the repression of senescence pathways that otherwise cause the premature depletion of stem cells.

[*Keywords*: Bmi-1; neural crest; stem cell; p16^{Ink4a}; p19^{Arf}; self-renewal]
[1]Correspondending author.
E-MAIL seanjm@umich.edu; FAX (734) 615-8133.
Article and publication are at http://www.genesdev.org/cgi/doi/10.1101/gad.1299505.

Results and Discussion

Like $p16^{Ink4a}$ (Molofsky et al. 2003), $p19^{Arf}$ expression increased in the absence of *Bmi-1*. $p19^{Arf}$ was not detected in the wild-type SVZ or cerebellum, but was detected in these tissues in the absence of *Bmi-1* (Fig. 1A). $p19^{Arf}$ was up-regulated in *Bmi-1*$^{-/-}$ CNS neurospheres cultured from the SVZ (Fig. 1B) and *Bmi-1*$^{-/-}$ PNS neurospheres cultured from the adult gut wall (data not shown), though $p19^{Arf}$ was also detected at lower levels in wild-type neurospheres. The detection of both $p16^{Ink4a}$ (Molofsky et al. 2003) and $p19^{Arf}$ in cultured neurospheres despite not detecting these proteins in vivo suggests that *Ink4a* and *Arf* are induced in wild-type cells in culture, though not to the extent as in *Bmi-1*$^{-/-}$ cells. This is consistent with our failure to detect *Ink4a* or *Arf* by PCR in uncultured wild-type NCSCs isolated by flow cytometry (Molofsky et al. 2003).

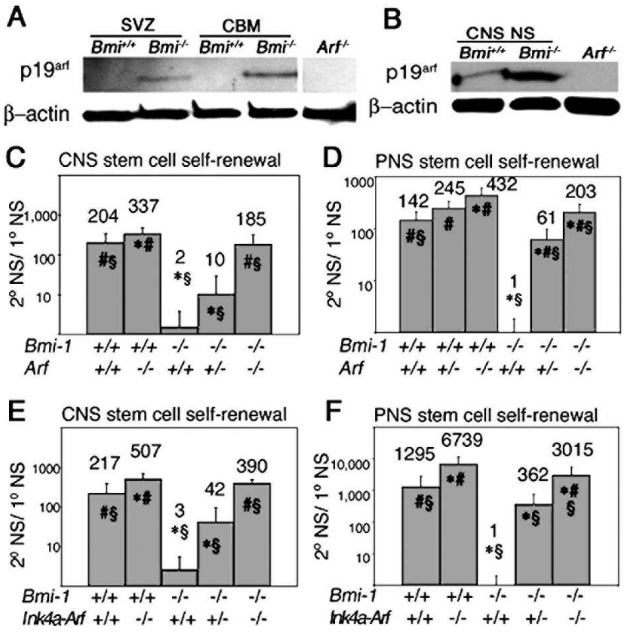

Figure 1. $p19^{Arf}$ is up-regulated in the absence of *Bmi-1*, and deletion of *Arf* or *Ink4a–Arf* significantly increased the self-renewal of neural stem cells from the SVZ and gut of *Bmi-1*$^{-/-}$ mice. (*A*) $p19^{Arf}$ was increased in uncultured SVZ and cerebellum (CBM) of 4-wk-old *Bmi-1*$^{-/-}$ mice. Western blot of neurosphere cells from *Arf*$^{-/-}$ mice is shown as a negative control. (*B*) $p19^{Arf}$ was increased in *Bmi-1*$^{-/-}$ CNS neurospheres (NS) cultured for 13 d. (*C*,*D*) *Arf* deficiency significantly increased self-renewal (the number of secondary neurospheres generated per subcloned primary neurosphere) within *Bmi-1*$^{+/+}$ and *Bmi-1*$^{-/-}$ CNS neurospheres (*C*) and PNS neurospheres (*D*), as well as the percentage of cells from *Bmi-1*$^{-/-}$ (but not *Bmi-1*$^{+/+}$) primary neurospheres that formed secondary neurospheres upon replating (Supplementary Fig. 6). CNS data represent mean ± SD for two to four mice per genotype, in four independent experiments. PNS data are from three to seven mice per genotype in four independent experiments. (*E*,*F*) *Ink4a–Arf* deficiency significantly increased self-renewal within *Bmi-1*$^{+/+}$ and *Bmi-1*$^{-/-}$ CNS neurospheres (*E*; mean ± SD for two to four mice per genotype, four independent experiments) and PNS neurospheres (*F*; three to six mice per genotype, six independent experiments), and the percentage of cells from *Bmi-1*$^{-/-}$ (but not *Bmi-1*$^{+/+}$) primary neurospheres that formed secondary neurospheres upon replating (Supplementary Fig. 6). (*) Significantly different ($P < 0.05$) from *Bmi-1*$^{+/+}$*Arf*$^{+/+}$ or *Bmi-1*$^{+/+}$*Ink4a–Arf*$^{+/+}$; (#) significantly different from *Bmi-1*$^{-/-}$*Arf*$^{+/+}$ or *Bmi-1*$^{-/-}$*Ink4a–Arf*$^{+/+}$; (§) significantly different from *Bmi-1*$^{+/+}$*Arf*$^{-/-}$ or *Bmi-1*$^{+/+}$*Ink4a–Arf*$^{-/-}$. All experiments were performed on 4- to 8-wk-old mice.

Arf deficiency significantly increased self-renewal within both *Bmi-1*$^{+/+}$ and *Bmi-1*$^{-/-}$ neurospheres from the CNS and PNS (Fig. 1C,D). The ability of *Arf* deficiency to increase the self-renewal of *Bmi-1*$^{+/+}$ neural stem cells in culture presumably reflects the fact that primary neurospheres were subcloned after 10 d in culture, well after $p19^{Arf}$ was induced in these cells. Since only about half as much self-renewal was observed within *Bmi-1*$^{-/-}$*Arf*$^{-/-}$ neurospheres as compared with *Bmi-1*$^{+/+}$*Arf*$^{-/-}$ neurospheres in the CNS and PNS, *Arf* deficiency appeared to only partially rescue the self-renewal of *Bmi-1*$^{-/-}$ neurospheres. Consistent with this, *Arf* deficiency also significantly increased the size of neurospheres (Supplementary Fig. 1B) and the percentage of cells within *Bmi-1*$^{-/-}$ neurospheres that could form secondary neurospheres (Supplementary Fig. 6B).

Deletion of *Ink4a* and *Arf* (*Ink4a–Arf*$^{-/-}$) significantly increased self-renewal within *Bmi-1*$^{+/+}$ and *Bmi-1*$^{-/-}$ neurospheres from the CNS and PNS (Fig. 1E,F). The rates of self-renewal suggested that *Ink4a–Arf* deficiency rescued most but not all of the *Bmi-1*$^{-/-}$ CNS self-renewal defect and about half of the PNS self-renewal defect (cf. *Bmi-1*$^{-/-}$*Ink4a–Arf*$^{-/-}$ vs. *Bmi-1*$^{+/+}$*Ink4a–Arf*$^{-/-}$ in Fig. 1E,F). More self-renewal was observed in Figure 1F than in Figure 1D because the neurospheres were cultured longer before subcloning. *Ink4a–Arf* deficiency also significantly increased the size of neurospheres (Supplementary Fig. 1C,D) and the percentage of cells within *Bmi-1*$^{-/-}$ neurospheres that could form secondary neurospheres (Supplementary Fig. 6C).

Ink4a, Arf, *or* Ink4a–Arf *deficiency partially rescue* Bmi-1$^{-/-}$ *neural stem cell frequency*

To test whether *Ink4a* deficiency could also rescue stem cell frequency in vivo, we cultured dissociated forebrain SVZ cells from 4- to 8-wk-old mice to determine the frequency of freshly dissociated cells that could form multipotent neurospheres. Cells were plated at clonal density, cultured for 10 d, then replated to adherent cultures for 3–5 d and stained for neurons, astrocytes, and oligodendrocytes. As observed previously, a significantly lower percentage of cells from the *Bmi-1*$^{-/-}$ SVZ formed multipotent neurospheres (Fig. 2). *Ink4a* deficiency significantly increased the percentage of *Bmi-1*$^{-/-}$ but not *Bmi-1*$^{+/+}$ SVZ cells that formed multipotent neurospheres (Fig. 2A). This is consistent with $p16^{Ink4a}$ expression in *Bmi-1*$^{-/-}$ but not in *Bmi-1*$^{+/+}$ SVZ cells in vivo (Molofsky et al. 2003). The magnitude of the increase suggested that *Ink4a* deficiency partially rescued stem cell frequency in the *Bmi-1*$^{-/-}$ SVZ.

We also cultured dissociated cells from the outer gut wall where NCSCs persist throughout adult life (Kruger et al. 2002). Cells were plated at clonal density, cultured for 10 d, then replated to adherent cultures for 5 d and stained for neurons, glia, and myofibroblasts. *Ink4a* deficiency significantly increased the percentage of *Bmi-1*$^{-/-}$ but not *Bmi-1*$^{+/+}$ cells that formed multipotent neurospheres (Fig. 2B). The magnitude of the increase again suggested that *Ink4a* deficiency partially rescued stem cell frequency in the *Bmi-1*$^{-/-}$ gut.

To confirm the partial rescue in neural stem cell frequency in vivo, we exploited our ability to prospectively identify uncultured NCSCs by flow cytometry based on their expression of high levels of the p75 neurotrophin receptor ($p75^{+}$ cells) (Bixby et al. 2002; Kruger et al.

2002). In these experiments, 30%–50% of p75$^+$ cells of all genotypes formed NCSC colonies in culture (data not shown), a 30- to 300-fold enrichment for NCSCs relative to unfractionated cells (0.1%–1.4% of unfractionated gut cells, depending on genotype, formed stem cell colonies in culture) (Fig. 2). The frequency of p75$^+$ cells was significantly reduced in the absence of *Bmi-1* (Fig. 3A,B). *Ink4a* deficiency had no effect on the frequency of p75$^+$ cells from *Bmi-1*$^{+/+}$ mice, but did significantly increase the frequency of p75$^+$ cells in *Bmi-1*$^{-/-}$ mice (Fig. 3C–E). The magnitude of the increase again suggested a partial rescue of *Bmi-1*$^{-/-}$ stem cell depletion. This analysis of prospectively identified, uncultured NCSCs was thus consistent with results from the functional assays in culture in indicating that Bmi-1 promotes the post-natal maintenance of neural stem cells partly by repressing *Ink4a*.

Arf deficiency (Fig. 2C,D) and *Ink4a–Arf* deficiency (Fig. 2E,F) also partly rescued the depletion of CNS and PNS stem cells in *Bmi-1*$^{-/-}$ mice, significantly increasing the percentage of freshly dissociated SVZ cells and outer gut wall cells from *Bmi-1*$^{-/-}$ but not *Bmi-1*$^{+/+}$ mice that formed multipotent neurospheres in culture. The percentages of SVZ and gut cells from *Bmi-1*$^{-/-}$*Ink4a–Arf*$^{-/-}$ and *Bmi-1*$^{+/+}$*Ink4a–Arf*$^{-/-}$ mice that formed multipotent neurospheres suggest that *Ink4a–Arf* deficiency rescued most of the CNS stem cell maintenance defect and about half of the *Bmi-1*$^{-/-}$ PNS stem cell maintenance defect. These results demonstrate that increased expression of $p16^{Ink4a}$ and $p19^{Arf}$ in the absence of Bmi-1 are responsible for much but not all of the neural stem cell self-renewal and maintenance defects observed in *Bmi-1*$^{-/-}$ mice.

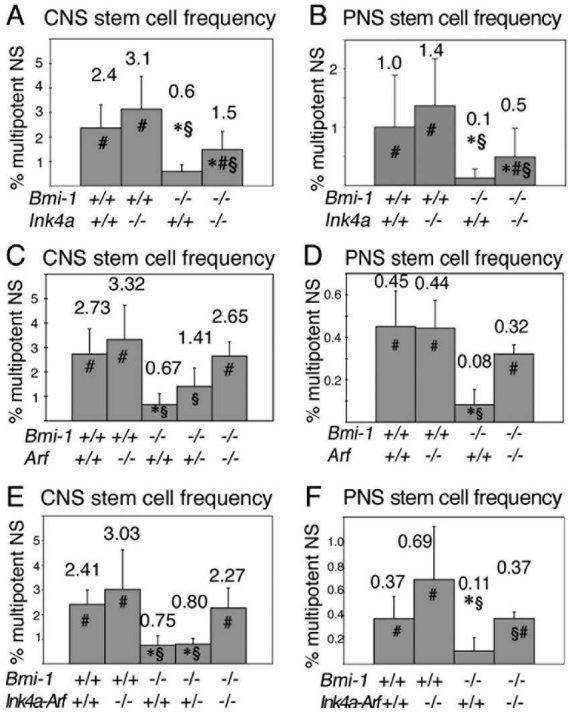

Figure 2. Deletion of *Ink4a*, *Arf*, or *Ink4a–Arf* significantly increased neural stem cell frequency in *Bmi-1*$^{-/-}$ mice. (*A*,*B*) *Ink4a* deficiency significantly increased the percentage of SVZ cells (*A*) or adult gut NCSCs (*B*) from *Bmi-1*$^{-/-}$ mice that formed multipotent neurospheres in culture (mean ± SD for four independent experiments). (*C*,*D*) *Arf* deficiency also significantly increased the percentage of *Bmi-1*$^{-/-}$ cells that formed multipotent neurospheres from the SVZ (*C*; three to six mice per genotype, in six independent experiments) or gut wall (*D*; four mice per genotype, in four independent experiments). (*E*,*F*) *Ink4a–Arf* deficiency significantly increased the frequency of cells from the *Bmi-1*$^{-/-}$ adult SVZ (*E*; two to seven mice per genotype, eight independent experiments) or gut wall (*F*; three to eight mice per genotype, three independent experiments) that formed multipotent neurospheres in culture. (*) Significantly different ($P < 0.05$ by *t*-test) from wild-type; (#) significantly different from *Bmi-1*$^{-/-}$*Ink4a*$^{+/+}$, *Bmi-1*$^{-/-}$*Arf*$^{+/+}$, or *Bmi-1*$^{-/-}$*Ink4a–Arf*$^{+/+}$; (§) significantly different from *Bmi-1*$^{+/+}$*Ink4a*$^{-/-}$, *Bmi-1*$^{+/+}$*Arf*$^{-/-}$, or *Bmi-1*$^{+/+}$*Ink4a–Arf*$^{-/-}$. All experiments employed 4- to 8-wk-old mice.

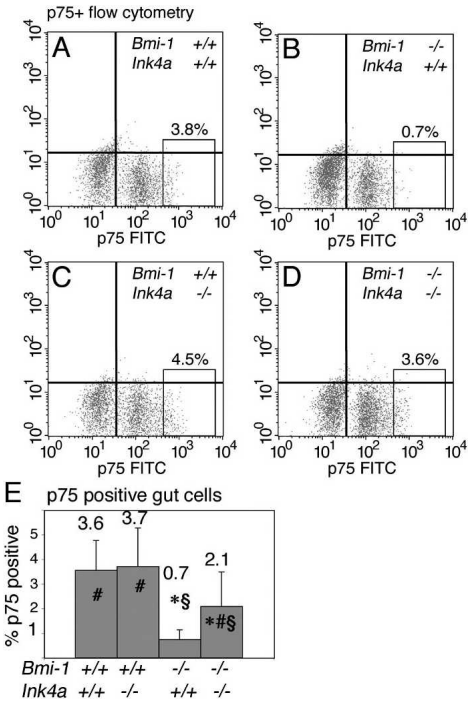

Figure 3. *Ink4a* deficiency partially rescued the frequency of uncultured NCSCs in the adult gut. *Ink4a* deficiency partially rescued the frequency of p75$^+$ cells, which are highly enriched for NCSCs, in the adult gut wall of *Bmi-1*$^{-/-}$ mice. (*A–D*) Representative flow-cytometry plots from the indicated genotypes demonstrating p75$^+$ NCSC frequency (boxed region of each plot) among freshly dissociated gut wall cells. (*E*) The frequency of p75$^+$ cells was significantly reduced by *Bmi-1* deficiency, and significantly increased by *Ink4a* deficiency. Data in panel *E* represent mean ± SD for 10 independent experiments using 4- to 8-wk-old mice. Statistical significance is indicated as in Figure 2.

Ink4a, Arf, *or* Ink4a–Arf *deficiency partially rescue neural development in* Bmi-1$^{-/-}$ *mice*

In the absence of *Bmi-1* there was a significant decline in the rate of proliferation (the percentage of cells that incorporated a pulse of BrdU) in the adult SVZ, where neurogenesis occurs in the forebrain (Fig. 4A). *Ink4a* deficiency had no effect on proliferation in the *Bmi-1*$^{+/+}$ forebrain (data not shown) but significantly increased proliferation in the *Bmi-1*$^{-/-}$ forebrain, suggesting a partial rescue of this phenotype (Fig. 4A). The number of myenteric plexus neurons per cross-section of the adult small intestine was significantly reduced in the absence of *Bmi-1* (Fig. 4B). *Ink4a* deficiency significantly increased the number of neurons per section through the *Bmi-1*$^{-/-}$ intestine (Fig. 4B). Thus *Ink4a* deficiency par-

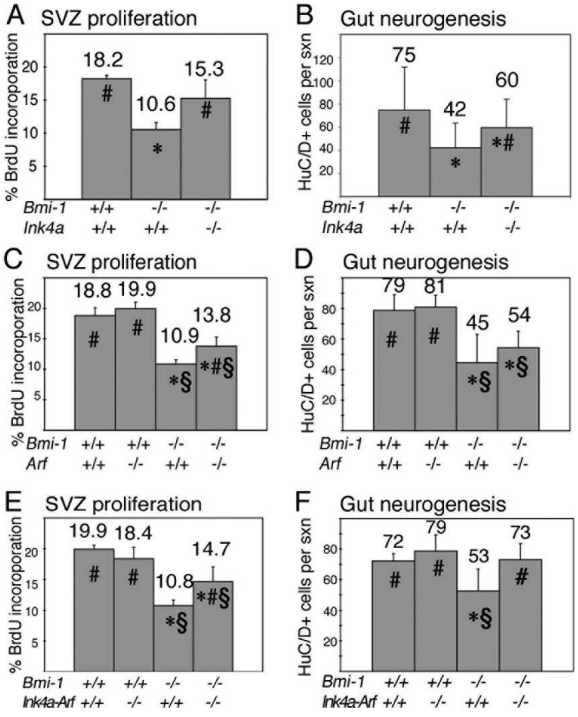

Figure 4. Deletion of *Ink4a*, *Arf*, or *Ink4a–Arf* partially rescued SVZ proliferation and gut neurogenesis in 3- to 9-wk-old *Bmi-1*$^{-/-}$ mice in vivo. (*A*,*C*,*E*) The rate of proliferation (percentage of cells that incorporate a pulse of BrdU) in the SVZ of *Bmi-1*$^{-/-}$ mice was significantly increased by *Ink4a* deficiency (*A*), *Arf* deficiency (*C*), or combined *Ink4a–Arf* deficiency (*E*). Note that deletion of these genes had no effect on SVZ proliferation in *Bmi-1*$^{+/+}$ mice (*C*,*E*; *Ink4a* data not shown; six to eight sections per mouse, three to five mice per genotype). *Ink4a* deficiency partially rescued the number of myenteric plexus neurons per cross-section through the distal small intestine of *Bmi-1*$^{-/-}$ mice (*B*; mean ± SD for four to seven mice per genotype, seven to 10 sections per mouse). *Arf* deficiency tended to increase the number of neurons per cross-section in *Bmi-1*$^{-/-}$ mice, though the effect was not statistically significant (*D*; mean ± SD for four to five mice per genotype and eight to 10 sections per mouse). *Ink4a–Arf* deficiency significantly increased the number of myenteric plexus neurons per cross-section of *Bmi-1*$^{-/-}$ mice in a way that was consistent with a complete rescue (*F*; mean ± SD for five mice per genotype and six to eight sections per mouse). (*) Significantly different ($P < 0.05$ by *t*-test) from wild-type; (#) significantly different from *Bmi-1*$^{-/-}$*Ink4a*$^{+/+}$, *Bmi-1*$^{-/-}$*Arf*$^{+/+}$, or *Bmi-1*$^{-/-}$*Ink4a–Arf*$^{+/+}$; (§) significantly different from *Bmi-1*$^{+/+}$*Arf*$^{-/-}$ or *Bmi-1*$^{+/+}$*Ink4a–Arf*$^{-/-}$.

tially rescued proliferation/neurogenesis in the forebrain and enteric nervous system of *Bmi-1*$^{-/-}$ mice.

Arf deficiency (Fig. 4C) or *Ink4a–Arf* deficiency (Fig. 4E) also significantly increased proliferation in the *Bmi-1*$^{-/-}$ but not *Bmi-1*$^{+/+}$ SVZ, suggesting partial rescues of this defect. *Arf* deficiency appeared to increase the number of neurons per section through the *Bmi-1*$^{-/-}$ small intestine, though the effect was not statistically significant (Fig. 4D). *Ink4a–Arf* deficiency significantly increased the number of neurons per section through the *Bmi-1*$^{-/-}$ but not *Bmi-1*$^{+/+}$ small intestine (Fig. 4F) to a degree consistent with a complete rescue. That some phenotypes (e.g., gut neurogenesis) appeared to be completely rescued by deleting *Ink4a* and *Arf*, while other phenotypes (e.g., SVZ proliferation) were only partially rescued indicates that the importance of other pathways downstream of Bmi-1 differs between regions of the nervous system.

Arf *or* Ink4a–Arf *deficiency partially rescue cerebellum development in* Bmi-1$^{-/-}$ *mice*

Bmi-1$^{-/-}$ mice exhibit morphologically smaller cerebellums, including significantly thinner granular and molecular cell layers and reduced cell density in the molecular layer (Fig. 5A–C; van der Lugt et al. 1994; Leung et al. 2004). *Ink4a–Arf* deficiency partially rescues cerebellum development in *Bmi-1*$^{-/-}$ mice (Jacobs et al. 1999a), though the relative importance of *Ink4a* and *Arf* in cerebellum development was not tested. Consistent with this prior report, we found that *Ink4a–Arf* deficiency had no effect on cerebellum development in *Bmi-1*$^{+/+}$ mice (data not shown), but did increase the overall cerebellum size in *Bmi-1*$^{-/-}$ mice, including significantly increasing the thickness of the granular and molecular layers, as well as cell density in the molecular layer (Fig. 5C). Nonetheless, all of these parameters remained significantly less than observed in wild-type littermates, indicating a partial rescue of cerebellum growth (Fig. 5C).

Ink4a deficiency had no effect on cerebellum development in *Bmi-1*$^{-/-}$ mice (Fig. 5A), despite the increased expression of $p16^{Ink4a}$ in the *Bmi-1*$^{-/-}$ cerebellum

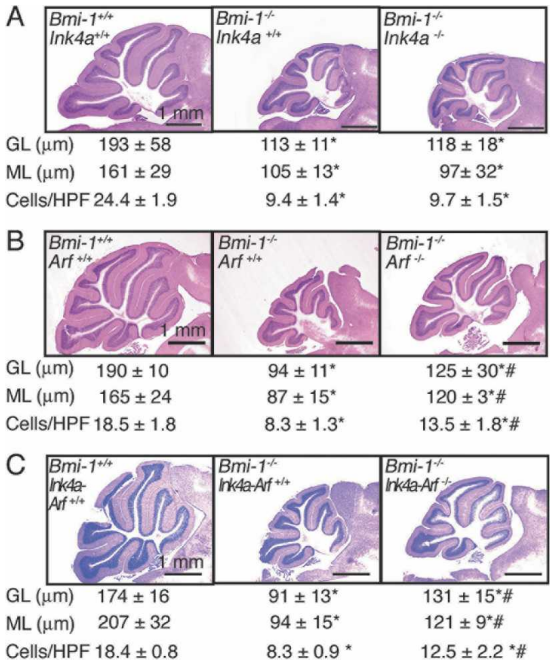

Figure 5. Deletion of *Arf* or *Ink4a–Arf*, but not *Ink4a* alone, partially rescues cerebellum development in *Bmi-1*$^{-/-}$ mice. Hematoxylin and eosin-stained saggital sections of adult cerebellum. Measurements of granular layer thickness (GL), molecular layer thickness (ML), and cell density in the molecular layer (cells/high power field [HPF] is 100 μm^2) for each genotype are represented *below* the corresponding picture. (*A*) *Ink4a* deficiency did not affect cerebellum development in *Bmi-1*$^{-/-}$ mice (mean ± SD for four mice per genotype, seven to 25 measurements per mouse). (*B*) *Arf* deficiency partially rescued cerebellum growth in 4- to 8-wk-old *Bmi-1*$^{-/-}$ mice (mean ± SD for three to four mice per genotype and 10–23 measurements per mouse). (*C*) *Ink4a–Arf* deficiency also partially rescued cerebellum growth in *Bmi-1*$^{-/-}$ mice (mean ± SD for three to five mice per genotype, six to 32 measurements per mouse). *Ink4a*, *Arf*, and *Ink4a–Arf* deficiencies did not affect cerebellum growth in *Bmi-1*$^{+/+}$ mice (data not shown). Statistical significance is indicated as in Figure 4.

(Supplementary Fig. 2). This suggests that progenitors from some regions of the nervous system can be insensitive to $p16^{Ink4a}$ expression. *Arf* deficiency had no effect on cerebellum development in *Bmi-1*$^{+/+}$ mice (data not shown) but increased the overall cerebellum size in *Bmi-1*$^{-/-}$ mice, in addition to significantly increasing the thickness of the granular and molecular layers, and cell density in the molecular layer (Fig. 5B), to a similar degree as observed from *Ink4a–Arf* deficiency (cf. Fig. 5C). The observation that *Arf* deficiency had a greater effect than *Ink4a* deficiency on cerebellum development in *Bmi-1*$^{-/-}$ mice indicates that the relative importance of $p16^{Ink4a}$ and $p19^{Arf}$ differs between progenitor populations and regions of the nervous system.

Ink4a, Arf, *or* Ink4a–Arf *deficiency do not rescue the growth or survival of* Bmi-1$^{-/-}$ *mice*

Although *Ink4a* deficiency, *Arf* deficiency, or *Ink4a–Arf* deficiency each partially rescued aspects of neural stem cell function and neural development in *Bmi-1*$^{-/-}$ mice, they did not affect the overall growth of *Bmi-1*$^{-/-}$ mice, which were significantly smaller than wild-type littermates (Supplementary Fig. 3). *Ink4a* deficiency or *Arf* deficiency also did not significantly affect brain mass in *Bmi-1*$^{-/-}$ mice (Supplementary Fig. 4A,B). *Ink4a–Arf* deficiency, on the other hand, did significantly increase brain mass in adult *Bmi-1*$^{-/-}$ mice, though only slightly (Supplementary Fig. 4C). The ability of *Ink4a* deficiency, *Arf* deficiency, and *Ink4a–Arf* deficiency to substantially rescue neural stem cell function while having little or no effect on brain growth in *Bmi-1*$^{-/-}$ mice indicates that the effects of Bmi-1 on neural stem cells can be uncoupled from effects on tissue growth.

Ink4a deficiency, *Arf* deficiency, or *Ink4a–Arf* deficiency also did not rescue the survival of *Bmi-1*$^{-/-}$ mice, which usually died by P30 (Supplementary Fig. 3), despite being born in nearly expected numbers (data not shown). *Ink4a–Arf* deletion did not prevent *Bmi-1*$^{-/-}$ mice from exhibiting ataxia (data not shown). Abnormalities in other tissues, such as the hematopoietic system, are also not completely rescued by *Ink4a–Arf* deletion and may exhibit less of a rescue than observed in the nervous system (see companion paper from Bruggeman et al. [2005]). It is likely that *Bmi-1*$^{-/-}$ mice have uncharacterized defects in the maintenance of other tissues that could also affect viability. Thus the early death of these mice is likely to derive from complex combinations of defects in multiple tissues.

It is difficult to precisely estimate the fraction of each phenotype rescued by *Ink4a* or *Arf* deletion; however, the extent to which *Ink4a–Arf* deficiency rescued SVZ proliferation (Fig. 4E) did not appear to be greater than observed from deletion of *Ink4a* (Fig. 4A) or *Arf* alone (Fig. 4C). Similarly, the extent to which *Ink4a–Arf* deficiency rescued neural stem cell frequency (Fig. 2E,F) appeared to be less than the sum of the effects of *Ink4a* deficiency (Fig. 2A,B) and *Arf* deficiency (Fig. 2C,D). This suggests that there is cross-regulation between the $p16^{Ink4a}$ and $p19^{Arf}$ pathways. A number of mechanisms by which the $p16^{Ink4a}$ and $p19^{Arf}$ pathways influence each other have already been identified (Lowe and Sherr 2003). For example, since $p21^{cip1}$, like $p16^{Ink4a}$, promotes Rb activation, changes in $p21^{cip1}$ expression affect the levels of $p16^{Ink4a}$ that are required to inhibit proliferation (Lowe and Sherr 2003). Consistent with this, we found that *cip1* RNA levels were reduced by *Arf* deficiency and increased by *Bmi-1* deficiency (as would be predicted based on the presumed changes in $p19^{Arf}$ and p53 activity in these cells) (Supplementary Fig. 4). These changes in *cip1* levels offer one possible source of cross-regulation that could account for the less-than-additive effects of *Ink4a* and *Arf* deletion, particularly given that $p21^{cip1}$ regulates neural stem cell self-renewal (Qiu et al. 2004; Kippin et al. 2005).

Ink4a and *Arf* repression represent important mechanisms by which Bmi-1 promotes post-natal stem cell self-renewal, stem cell maintenance, and development in the nervous system. Since induction of $p16^{Ink4a}$ and $p19^{Arf}$ have been associated with cellular senescence (Lowe and Sherr 2003), neural stem cells appear to undergo premature senescence in the absence of Bmi-1 and become depleted by adulthood. This suggests that the repression of these senescence pathways is a fundamental requirement for the maintenance of neural stem cells throughout life.

Materials and methods

The *Bmi-1*$^{+/-}$, *Arf*$^{+/-}$, and *Ink4a–Arf*$^{+/-}$ mice were backcrossed at least eight times onto a C57BL background. Initial experiments employed *Ink4a*$^{+/-}$ mice on an FvB background, but all results were subsequently confirmed using *Ink4a*$^{+/-}$ mice backcrossed five times onto a C57BL background. All mice were genotyped by PCR using primers described in the Supplemental Material.

Isolation of CNS and PNS progenitors

Adult SVZ was obtained by coronally sectioning brains in ice-cold Opti-MEM medium (Gibco). The lateral walls of the lateral ventricles were removed, minced, then dissociated for 20 min at 37°C in 0.025% trypsin/0.5 mM EDTA (Calbiochem) plus 0.001% DNase1 (Roche). Cells were quenched with staining medium (L15 medium containing 1 mg/mL BSA [Sigma A-3912], 10 mM HEPES at pH 7.4, and 1% penicillin/streptomycin [BioWhittaker]) containing 0.014% soybean trypsin inhibitor (Sigma) and 0.001% DNase1. After centrifuging, the cells were resuspended in staining medium, triturated, filtered through nylon screen (45 µm, Sefar America), counted by hemocytometer, and plated.

For PNS progenitor isolation, adult mouse guts were dissected into ice-cold PBS. Outer muscle/plexus layers were peeled free from the underlying epithelium as described (Kruger et al. 2002), then minced, and dissociated for 45 min in 0.025% trypsin/EDTA (Gibco 25300-054) plus 1 mg/mL type 4 collagenase (Worthington) in Ca, Mg-free HBSS at 37°C with agitation every 5 min. The dissociated cells were then quenched in staining medium, resuspended, and filtered as described above. Dissociated gut cells were sometimes stained with an antibody against p75 (Ab 1554; Chemicon International) as described previously (Bixby et al. 2002). The analysis and sorting of $p75^+$ cells was performed by a FACS VantageSE flow cytometer (Becton-Dickinson).

Cell culture and self-renewal assay

Cells were plated at clonal density (2000 cells per well of a six-well plate; 1.3 cells/µL of culture medium) on ultra-low binding plates (Corning) to grow neurospheres. Culture medium was based on a 5:3 mixture of DMEM-low glucose: neurobasal medium (Gibco) supplemented with 20 ng/mL human bFGF (R&D Systems), 1% N2 supplement (Gibco), 2% B27 supplement (Gibco), 50 µM 2-mercaptoethanol, and 1% pen/strep (Biowhittaker). CNS cultures also contained 20 ng/mL EGF (R&D Systems) and 10% chick embryo extract (prepared as described [Stemple and Anderson 1992]). PNS cultures contained 15% chick embryo extract, 35 mg/mL (110 nM) retinoic acid (Sigma), and 20 ng/mL IGF1 (R&D Systems). All cultures were maintained at 37°C in 6% CO_2/balance air.

To measure self-renewal, individual CNS neurospheres were dissociated by trituration, then replated at clonal density in nonadherent cultures. Secondary neurospheres were counted 5–10 d later to determine the number of secondary neurospheres formed per primary neurosphere. Individual PNS neurospheres were replated for 48 h into adherent plates to allow the spheres to spread out over the culture dish. The adherent colonies were then treated with trypsin and collagenase (four parts 0.05%

trypsin-EDTA plus one part 10 mg/mL collagenase IV) for 5 min at 37°C followed by trituration. Five thousand dissociated cells were replated per well of a six-well plate and secondary neurospheres were counted 10 d later.

Western blots, qRT–PCR, and immunohistochemistry were performed as described in the Supplemental Material.

Acknowledgments

Thanks to David Adams, Anne Marie Deslaurier, and the University of Michigan Flow-Cytometry Core Facility (supported by UM-Comprehensive Cancer NIH CA46592, and UM-Multipurpose Arthritis Center NIH P60-AR20557). Thanks to Elizabeth Smith in the Hybridoma Core Facility (supported through the Michigan Diabetes Research and Training Center, NIH5P60-DK20572, and the Rheumatic Disease Center, P30 AR48310). Thanks to Kelly Yeager for tissue sectioning. Thanks to Maarten van Lohuizen for providing *Bmi-1*$^{+/-}$ mice and for sharing unpublished results, to Charles Sherr for providing *Arf*$^{+/-}$ mice, and to Ronald DePinho for providing *Ink4a*$^{+/-}$ and *Ink4a–Arf*$^{+/-}$ mice. This work was supported by the National Institutes of Health (R01 NS40750), the James S. McDonnell Foundation, and the Howard Hughes Medical Institute. A.V.M. was supported by a National Research Service Award from NIH (F30 NS048642). R.P. was supported by a post-doctoral fellowship from the Spanish Ministry of Science and Technology. S.H. was supported by a fellowship from the University of Michigan Cellular and Molecular Biology program.

References

Bixby, S., Kruger, G.M., Mosher, J.T., Joseph, N.M., and Morrison, S.J. 2002. Cell-intrinsic differences between stem cells from different regions of the peripheral nervous system regulate the generation of neural diversity. *Neuron* **35:** 643–656.

Bruggeman, S.W.M., Valk-Lingbeek, M.E., van der Stoop, P.P.M., Jacobs, J.J.L., Kieboom, K., Tanger, E., Hulsman, D., Leung, C., Arsenijevic, Y., Marino, S., and van Lohuizen, M. 2005. *Ink4a* and *Arf* differentially affect cell proliferation and neural stem cell self-renewal in *Bmi1*-deficient mice. *Genes & Dev.* (this issue).

Dimri, G.P., Martinez, J.L., Jacobs, J.J., Keblusek, P., Itahana, K., van Lohuizen, M., Campisi, J., Wazer, D.E., and Band, V. 2002. The Bmi-1 oncogene induces telomerase activity and immortalizes human mammary epithelial cells. *Cancer Res.* **62:** 4736–4745.

Harrison, D.E. 1979. Proliferative capacity of erythropoietic stem cell lines and aging: An overview. *Mech. Ageing Dev.* **9:** 409–426.

Itahana, K., Zou, Y., Itahana, Y., Martinez, J.-L., Beausejour, C., Jacobs, J.J.L., van Lohuizen, M., Band, V., Campisi, J., and Dimri, G.P. 2003. Control of the replicative life span of human fibroblasts by p16 and the polycomb protein Bmi-1. *Mol. Cell. Biol.* **23:** 389–401.

Jacobs, J.J.L., Kieboom, K., Marino, S., DePinho, R.A., and van Lohuizen, M. 1999a. The oncogene and polycomb-group gene bmi-1 regulates cell proliferation and senescence through the ink4a locus. *Nature* **397:** 164–168.

Jacobs, J.J.L., Scheijen, B., Voncken, J.-W., Kieboom, K., Berns, A., and van Lohuizen, M. 1999b. Bmi-1 collaborates with c-Myc in tumorigenesis by inhibiting c-Myc-induced apoptosis via INK4a/ARF. *Genes & Dev.* **13:** 2678–2690.

Kamijo, T., Zindy, F., Roussel, M.F., Quelle, D.E., Downing, J.R., Ashmun, R.A., Grosveld, G., and Sherr, C.J. 1997. Tumor suppression at the mouse INK4a locus mediated by the alternative reading frame product p19ARF. *Cell* **91:** 649–659.

Kippin, T.E., Martens, D.J., and van der Kooy, D. 2005. p21 loss compromises the relative quiescence of forebrain stem cell proliferation leading to exhaustion of their proliferation capacity. *Genes & Dev.* **19:** 756–767.

Kruger, G.M., Mosher, J.T., Bixby, S., Joseph, N., Iwashita, T., and Morrison, S.J. 2002. Neural crest stem cells persist in the adult gut but undergo changes in self-renewal, neuronal subtype potential, and factor responsiveness. *Neuron* **35:** 657–669.

Lessard, J. and Sauvageau, G. 2003. Bmi-1 determines the proliferative capacity of normal and leukemic stem cells. *Nature* **423:** 255–260.

Lessard, J., Baban, S., and Sauvageau, G. 1998. Stage-specific expression of Polycomb Group genes in human bone marrow cells. *Blood* **91:** 1216–1224.

Leung, C., Lingbeek, M., Shakhova, O., Liu, J., Tanger, E., Saremaslani, P., van Lohuizen, M., and Marino, S. 2004. Bmi1 is essential for cerebellar development and is overexpressed in human medulloblastomas. *Nature* **428:** 337–341.

Lowe, S.W. and Sherr, C.J. 2003. Tumor suppression by Ink4a–Arf: Progress and puzzles. *Curr. Opin. Genet. Dev.* **13:** 77–83.

Maslov, A.Y., Barone, T.A., Plunkett, R.J., and Pruitt, S.C. 2004. Neural stem cell detection, characterization, and age-related changes in the subventricular zone of mice. *J. Neurosci.* **24:** 1726–1733.

Molofsky, A.V., Pardal, R., Iwashita, T., Park, I.K., Clarke, M.F., and Morrison, S.J. 2003. Bmi-1 dependence distinguishes neural stem cell self-renewal from progenitor proliferation. *Nature* **425:** 962–967.

Molofsky, A.V., Pardal, R., and Morrison, S.J. 2004. Diverse mechanisms regulate stem cell self-renewal. *Curr. Opin. Cell Biol.* **16:** 700–707.

Morrison, S.J., Wandycz, A.M., Akashi, K., Globerson, A., and Weissman, I.L. 1996. The aging of hematopoietic stem cells. *Nat. Med.* **2:** 1011–1016.

Morrison, S.J., Shah, N.M., and Anderson, D.J. 1997. Regulatory mechanisms in stem cell biology. *Cell* **88:** 287–298.

Park, I.-K., Qian, D., Kiel, M., Becker, M., Pihalja, M., Weissman, I.L., Morrison, S.J., and Clarke, M. 2003. Bmi-1 is required for the maintenance of adult self-renewing hematopoietic stem cells. *Nature* **423:** 302–305.

Qiu, J., Takagi, Y., Harada, J., Rodrigues, N., Moskowitz, M.A., Scadden, D.T., and Cheng, T. 2004. Regenerative response in ischemic brain restricted by p21cip1/waf1. *J. Exp. Med.* **199:** 937–945.

Serrano, M., Lee, H., Chin, L., Cordon-Cardo, C., Beach, D., and DePinho, R.A. 1996. Role of the INK4a locus in tumor suppression and cell mortality. *Cell* **85:** 27–37.

Sharpless, N.E., Bardeesy, N., Lee, K.-H., Carrasco, D., Castrillon, D.H., Aguirre, A.J., Wu, E.A., Horner, J.W., and DePinho, R.A. 2001. Loss of p16Ink4a with retention of p19Arf predisposes mice to tumorigenesis. *Nature* **413:** 86–91.

Sherr, C.J. 2001. The INK4a/ARF network in tumour suppression. *Nat. Rev. Mol. Cell Biol.* **2:** 731–737.

Stemple, D.L. and Anderson, D.J. 1992. Isolation of a stem cell for neurons and glia from the mammalian neural crest. *Cell* **71:** 973–985.

Valk-Lingbeek, M.E., Bruggeman, S.W., and van Lohuizen, M. 2004. Stem cells and cancer: The polycomb connection. *Cell* **118:** 409–418.

van der Lugt, N.M.T., Domen, J., Linders, K., van Roon, M., Robanus-Maandag, E., te Riele, H., van der Valk, M., Deschamps, J., Sofroniew, M., van Lohuizen, M., et al. 1994. Posterior transformation, neurological abnormalities, and severe hematopoietic defects in mice with a targeted deletion of the bmi-1 proto-oncogene. *Genes & Dev.* **8:** 757–769.